

A GRAPHICALLY INTEGRABLE PREDICTION MODEL INCORPORATING OROGRAPHIC INFLUENCES

By *Mariano A. Estoque*

University of Chicago^{1,2}

(Manuscript received 15 November 1956)

ABSTRACT

An attempt to incorporate the effect of sloping terrain in a two-level model is presented. The resulting prediction equations may be integrated by graphical techniques. To derive the equations, it is necessary to prescribe an analytic expression for the vertical velocity profile. An actual forecast made with use of the model indicates that considerable improvement may be obtained over forecasts based on models which do not take into account orographic effects.

1. Introduction

Recent tests of a graphical integration model (Estoque, 1957; Petterssen *et al.*, 1957) have shown that the error patterns of the sea-level prognoses over North America are closely related to the topography of the Rocky Mountains. Almost identical patterns were found by Thompson and Gates (1956) in their numerical integrations based upon the thermotropic model. These patterns also appear to repeat themselves in numerical integrations of the three-level model currently provided by the U. S. Joint Numerical Weather Prediction Unit. One is thus led to the conclusion that the patterns of orographic errors are important in the dynamical models tested so far.

In the above-mentioned models one has to assume, as a boundary condition, that the vertical velocity vanishes at the bottom of the atmosphere. The purpose of this article is to extend a model previously described (Estoque, 1957) so as to incorporate orographic effects in such a manner that the prediction equations can still be integrated graphically.

2. The prediction equations

The characteristics of the basic model having been previously described in the article just cited, it suffices here to account for the additional terms which represent the effects of vertical motions induced by sloping terrain. Pressure (p) will be used as a vertical coordinate, and the vertical velocity, dp/dt , will be denoted by ω . Subscripts 0, L , and c will denote values at the 1000-mb surface, the level of non-divergence (500 mb), and the middle level $p_c = (p_0 + p_L)/2$, respectively.

The vertical velocity distribution will be assumed

to be a linear combination of two terms such that

$$\omega(x, y, p, t) = N(x, y, t) n(p) + R(x, y, t) r(p). \quad (1)$$

Here $N(x, y, t) n(p)$ represents the distribution of ω if no orographic influences were present, while the term $R(x, y, t) r(p)$ represents the orographically-forced vertical velocity component. The symbols are defined as

$$n \equiv \sin \left[\frac{\pi}{2} \frac{p_0 - p}{p_0 - p_L} \right], \quad r \equiv \left(\frac{p}{p_0} \right)^b,$$

$R \equiv -g\rho_0 V_0 \cdot \nabla H$, $g \equiv$ acceleration of gravity, $\rho_0 \equiv$ density of the air at the 1000-mb level, and $H \equiv$ elevation of the ground above sea level.

The velocity V_0 is assumed to be the geostrophic wind at 1000 mb, while b is a positive number which may be determined empirically. The orographically-induced vertical velocity has a numerical maximum at the bottom, which is equal to the vertical component of the upslope or downslope motion, and decreases monotonically to zero at the top of the atmosphere. The rate of decrease is proportional to the parameter b . In the absence of sloping terrain ($\nabla H \equiv 0$), the second term vanishes and (1) reduces to the distribution used previously in the basic model. The postulated distribution along the vertical of the vertical velocity cannot readily be justified with reference to dynamical principles, although the observed effects of orography on large-scale motions appear to imply such a distribution.

If the foregoing expression for ω is incorporated in the simplified quasi-geostrophic vorticity equation and in the thermodynamic energy equation for adiabatic motion (applied at level c on the assumption that the hodograph is straight),

$$\frac{d}{dt} \left(\frac{g}{f} \nabla^2 z + f \right) = f \frac{\partial \omega}{\partial p}$$

¹ The research was made possible through support and sponsorship extended by the Geophysics Research Directorate, Air Force Cambridge Research Center, under Contract No. AF19(604)-1293.

² Present Affiliation: McGill University.

and

$$\frac{d}{dt} \left(\frac{\partial z}{\partial p} \right) + \sigma\omega = 0,$$

the following expressions are obtained:

$$\frac{d}{dt} \left(\frac{g}{f} \nabla^2 z + f \right) = f \left(N \frac{\partial n}{\partial p} + R \frac{\partial r}{\partial p} \right), \quad (2)$$

and

$$\frac{d}{dt} (z_L - z_0) = (Nn_c + Rr_c)(p_0 - p_L)\sigma_c, \quad (3)$$

where

$$\frac{d}{dt} \equiv \frac{\partial}{\partial t} + V \cdot \nabla, \quad \sigma \equiv \frac{1}{\theta} \frac{\partial z}{\partial p} \frac{\partial \theta}{\partial p},$$

$\theta \equiv$ potential temperature,

$$\nabla \equiv i \frac{\partial}{\partial x} + j \frac{\partial}{\partial y},$$

and $V \equiv$ geostrophic wind.

Now, eliminating N , one obtains

$$\frac{d}{dt} \left[\frac{g}{f} \nabla^2 z + f - \psi(z_L - z_0) \right] + \mu V_0 \cdot \nabla H = 0. \quad (4)$$

Here

$$\psi \equiv \frac{f \partial n / \partial p}{\sigma_c n_c (p_0 - p_L)},$$

and

$$\mu \equiv g \rho_0 f \left(\frac{\partial r}{\partial p} - \frac{r_c}{n_c} \frac{\partial n}{\partial p} \right).$$

In the derivation of (4), the variation of f in the right-hand side of (2) has been neglected. If (4) is applied at level $p = p_0$ and then at level $p = p_L$, one obtains

$$(d/dt)_0(z_L - Bz_L - z_0 + MH) = 0, \quad (5)$$

and

$$(d/dt)_L(z_L - \bar{z}_L - G - EH) = 0. \quad (6)$$

Here the Laplacian is replaced by finite differences,

$$B \equiv \left[1 + \frac{\pi f^2 d^2}{(32)^{0.5} g m^2 (z_L - z_0)_s \log(\theta_L/\theta_0)_s} \right]^{-1}$$

is taken as a constant to be computed from the standard atmosphere (subscript s),

$$G \equiv \int_0^\phi \frac{d^2 f^2}{4 g m^2} \cot \phi \, d\phi,$$

$$M \equiv \frac{B f^2 d^2 \rho_0}{4 m^2 n_c} \left[n_c \left(\frac{\partial r}{\partial p} \right)_0 - r_c \left(\frac{\partial n}{\partial p} \right)_0 \right],$$

$$E \equiv \frac{a f^2 d^2 \rho_0}{4 m^2} \left(\frac{\partial r}{\partial p} \right)_L,$$

$m \equiv$ map-scale factor,

and

$$\bar{z} \equiv [z(x-d) + z(x+d) + z(y-d) + z(y+d)]/4.$$

In arriving at (5) from (4), the variations of m^2/f , f^2/m^2 and Bz_0 are assumed to be small. Furthermore, in (6), the velocity V_0 has been replaced by aV_L to obtain a conservation equation; this artifice has been used by Charney and Eliassen (1949), who suggested the value $a \approx 0.4$.

It will be seen from (5) and (6) that the orographic influences are represented in the terms involving M and E . Apart from being functions of certain physical and geometrical quantities, M and E depend upon the empirical factor b , which is proportional to the rate of decrease with height of the orographically-forced vertical motion. This dependence is shown in table 1. The number $(p_L/p_0)^b$ represents the ratio of the orographically-induced vertical velocity at 500 mb to that at 1000 mb.

Examination of table 1 reveals that the predicted 1000-mb height changes are relatively insensitive to the assumed value of the parameter b . Thus the changes depend mainly on the magnitude of the vertical velocities associated with downslope or upslope motions at the bottom of the atmosphere, not on their decrease with height. For the examples presented in the following section, the values used for M and E are 0.07 and 0.01, respectively, which correspond to a value of b between 2 and 3. Further experimentation would indicate the optimum value of b .

The physical interpretation of the prediction equations may be seen more easily by writing them in the form

$$\frac{\partial}{\partial t} (z_L - Bz_L - z_0) = -V_0 \cdot \nabla (z_L - Bz_L - z_0) - MV_0 \cdot \nabla H, \quad (7)$$

and

$$\frac{\partial}{\partial t} (z_L - \bar{z}_L - G) = -V_L \cdot \nabla (z_L - \bar{z}_L - G) + EV_L \cdot \nabla H. \quad (8)$$

The quantity $z_L - Bz_L - z_0$ is (since $B \approx 0.5$ in middle latitudes) approximately equal to the thickness from 1000 to 750 mb. Therefore, the inclusion of the last term on the left of (7) implies that downslope (upslope) motion results in a local increase (decrease) in the thickness. Similarly, the term on the left of (8)

TABLE 1. Values of M , E , and $(p_L/p_0)^b$ as functions of b . ($B = 0.5$, $f = 10^{-4} \text{ sec}^{-1}$, $d = 1000 \text{ km}$, $\rho_0 = 1.2 \times 10^{-3} \text{ g/cm}^3$, $p_L = 500 \text{ mb}$, $a = 0.4$, $m = 1$.)

b :	1	2	3	4	5
M :	0.064	0.067	0.072	0.081	0.091
E :	0.012	0.012	0.009	0.006	0.004
$(p_L/p_0)^b$:	0.50	0.25	0.12	0.06	0.03

is approximately equal to the local change of the 500-mb height (since the variation of \bar{z}_L is small, and G is constant locally) and the effect of orography is to cause 500-mb falls (rises) downwind (upwind).

The falls at 500 mb and the increased thicknesses in the lee of mountain ranges combine hydrostatically to produce height falls in the 1000-mb surface; cyclonic development is indicated when the Laplacian of the 1000-mb falls is positive. The mechanism visualized here is similar to that discussed in a general manner by Petterssen (1950), and his statistics on lee developments confirm that the mechanism is significant.

If the terms on the right are expressed in the form of Jacobians, the final prediction equations may be written as

$$\frac{\partial}{\partial t} (z_L - Bz_L - z_0 + MH) = -\frac{g}{f} J(z_L - Bz_L + MH, z_L - Bz_L - z_0 + MH), \quad (9)$$

and

$$\frac{\partial}{\partial t} (z_L - \bar{z}_L - G - EH) = -\frac{g}{f} J(\bar{z}_L + G + EH, z_L - \bar{z}_L - G - EH). \quad (10)$$

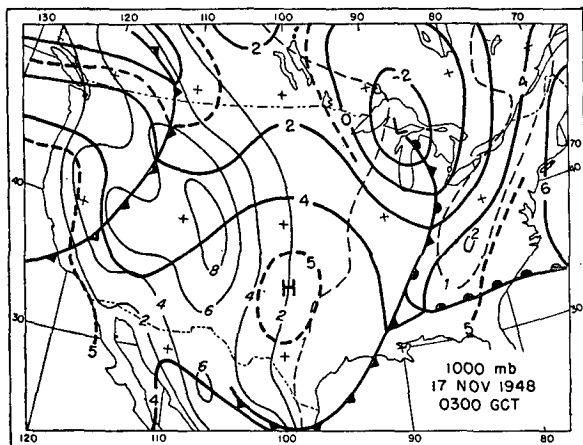


FIG. 1. Initial 1000-mb chart. Heavy lines are isobaric contour heights in hundreds of feet; thin lines represent elevations of topography in thousands of feet.

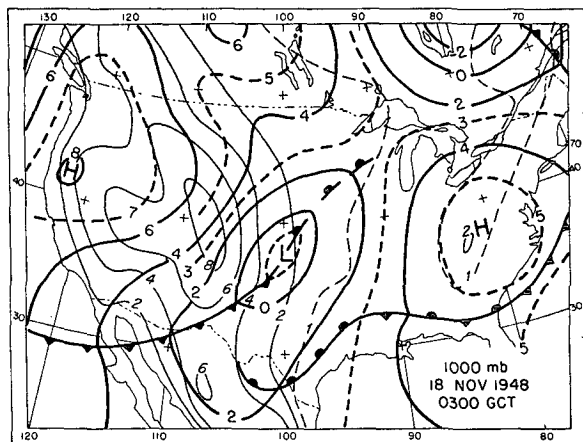


FIG. 2. Verifying 1000-mb chart. Heavy lines are isobaric contours in hundreds of feet. Thin lines represent elevations of topography in thousands of feet.

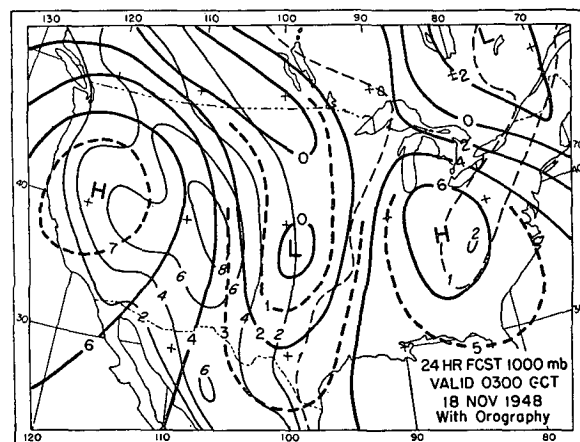


FIG. 4. Graphical forecast with orography. Heavy lines are isobaric contours in hundreds of feet. Thin lines represent elevations of topography in thousands of feet.

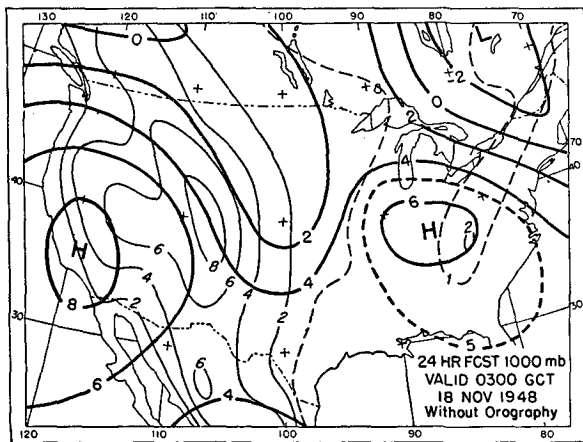


FIG. 3. Graphical forecast without orography. Heavy lines are isobaric contour heights in hundreds of feet; thin lines represent elevations of topography in thousands of feet.

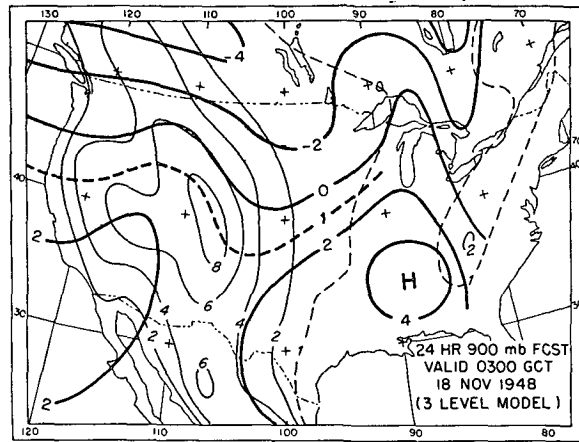


FIG. 5. Three-level numerical forecast without orography. Heavy lines are D -values of 900-mb surface in hundreds of feet. Thin lines represent elevations of topography in thousands of feet.

A simple procedure for making forecasts of z_L and z_0 , with use of a relatively large smoothing distance d , such as 1000 km, is as follows:

1. By means of graphical additions and subtractions, construct the $z_L - \bar{z}_L - G - EH$ and $\bar{z}_L + G + EH$ field using the initial z_L chart.

2. Advect the former, using the latter as the advecting field. The advected field represents the forecast $z_L - \bar{z}_L - G - EH$.

3. For large smoothing distances, the changes in \bar{z}_L are generally much smaller than those of z_L . The forecast z_L is, therefore, obtained by adding the initial $\bar{z}_L + G + EH$ field to the advected $z_L - \bar{z}_L - G - EH$ field (step 2).

4. Construct the $z_L - Bz_L - z_0 + MH$ and the $z_L - Bz_L + MH$ fields by graphical additions and subtractions, using the initial z_0 and z_L charts.

5. Advect the former, using the latter as the advecting field. The advected field represents the forecast for $z_L - Bz_L - z_0 + MH$.

6. Using the forecast z_L field, construct the forecast $z_L - Bz_L + MH$ field.

7. Subtract the result of step 5 from that of step 6, to obtain the forecast z_0 field.

In the advection process, both advecting fields are assumed to be geostrophic and stationary. The z_L forecast obtained in step 3 does not take into account the changes in the \bar{z}_L field during the forecast period. To minimize errors from this source (use of the initial instead of the forecast $\bar{z}_L + G + EH$), one may construct a first approximation to the forecast $\bar{z}_L + G + EH$ field using the predicted z_L in step 3. This approximate forecast for $\bar{z}_L + G + EH$ is then added to the forecast $z_L - \bar{z}_L - G - EH$ in step 2, to obtain a better z_L forecast.

3. An example

To determine whether the prediction equations, (9) and (10), possess any ability to account for orographic effects, we have chosen to apply them to a case of lee development investigated by Newton (1956), where it was indicated that orographic influence was prominent. For comparison, a 24-hr forecast was made with the above-mentioned graphical model without the orographic terms. The two forecasts thus obtained

TABLE 2. Correlation coefficients between observed and forecast 24-hr height changes.

Initial time	Graphical (1000 mb) Without orography	Graphical (1000 mb) With orography	3-level model (900 mb)
0300 GCT 17 Nov. 1948	0.36	0.72	0.20

have also been compared with the 24-hr forecast obtained by the three-level model without orographic influences. In arriving at the first of the above-mentioned forecasts, the generalized topography computed by Newton was used. The elevations represent average values over squares having sides equal to 300 km. The graphical forecasts were obtained by iteration in two 12-hr steps. The results are shown in figs. 1 to 5 and table 2.

It will be seen that the incorporation of orographic influences resulted in considerable improvement over the other forecasts without such influences. In the case investigated, it was known that the orographic influences appear to be strong. Whether the model will serve equally well in general can be determined with more extensive tests.

Acknowledgments.—The writer is grateful to Profs. Sverre Petterssen, George Platzman, and Chester Newton for helpful criticisms.

REFERENCES

- Charney, J. G., and A. Eliassen, 1949: A numerical method for predicting the perturbations of the middle latitude westerlies. *Tellus*, **1**, 38–54.
- Estoque, M. A., 1957: Graphical integrations of a two-level model. *J. Meteor.*, **14**, 50–54.
- Newton, C. W., 1956: Mechanisms of circulation change during a lee cyclogenesis. *J. Meteor.*, **13**, 528–539.
- Petterssen, S. P., 1950: Some aspects of the general circulation of the atmosphere. *Cent. Proc. r. meteor. Soc.*, 120–155.
- , M. A. Estoque, and L. Hughes, 1957: An experiment in prognostication. *J. Meteor.*, **14**, to be published.
- Thompson, P. D., and W. L. Gates, 1956: A test of numerical prediction methods based on the barotropic and two-parameter baroclinic models. *J. Meteor.*, **13**, 127–141.